

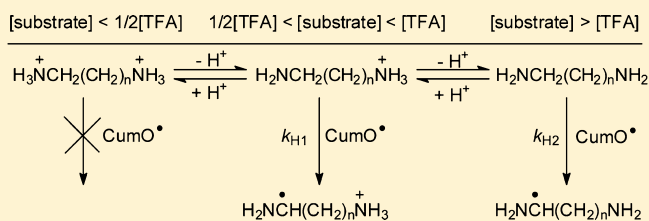
# Hydrogen Atom Transfer from 1,*n*-Alkanediamines to the Cumyloxy Radical. Modulating C–H Deactivation Through Acid–Base Interactions and Solvent Effects

Michela Milan, Michela Salamone, and Massimo Bietti\*

Dipartimento di Scienze e Tecnologie Chimiche, Università “Tor Vergata”, Via della Ricerca Scientifica, 1 I-00133 Rome, Italy

**S** Supporting Information

**ABSTRACT:** A time-resolved kinetic study on the effect of trifluoroacetic acid (TFA) on the hydrogen atom transfer (HAT) reactions from 1,*n*-alkanediamines ( $R_2N(CH_2)_nNR_2$ ,  $R = H, CH_3$ ;  $n = 1-4$ ), piperazine, and 1,4-dimethylpiperazine to the cumyloxy radical ( $CumO^\bullet$ ), has been carried out in MeCN and DMSO. Very strong deactivation of the  $\alpha$ -C–H bonds has been observed following nitrogen protonation and the results obtained have been explained in terms of substrate basicity, of the distance between the two basic centers and of the solvent hydrogen bond acceptor ability. At  $[substrate] \leq 1/2 [TFA]$  the substrates exist in the doubly protonated form  $HR_2N^+(CH_2)_nN^+R_2H$ , and no reaction with  $CumO^\bullet$  is observed. At  $1/2 [TFA] < [substrate] \leq [TFA]$ , HAT occurs from the C–H bonds that are  $\alpha$  to the nonprotonated nitrogen in  $R_2N(CH_2)_nN^+R_2H$ . At  $[substrate] > [TFA]$ , HAT occurs from the  $\alpha$ -C–H bonds of  $R_2N(CH_2)_nNR_2$ , and the measured  $k_{H1}$  values are very close to those obtained in the absence of TFA. Comparison between MeCN and DMSO clearly shows that in the monoprotonated diamines  $R_2N(CH_2)_nN^+R_2H$  remote C–H deactivation can be modulated through solvent hydrogen bonding.

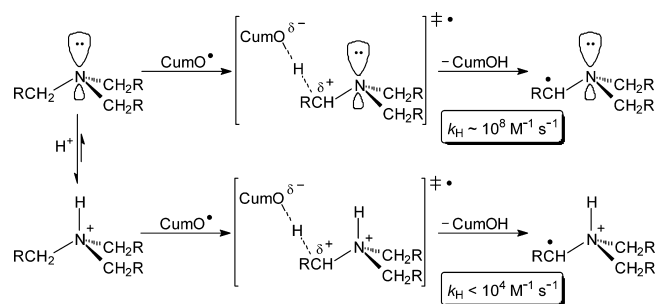


## INTRODUCTION

Synthetic procedures based on hydrogen atom transfer (HAT) from aliphatic C–H bonds to radical or radical-like species have attracted considerable interest as they can provide convenient methods for selective C–H functionalization.<sup>1–8</sup> In this context, a procedure that allows for control over HAT reactivity and selectivity through C–H deactivation has been recently described by our research group, and exploits the effect of acid–base interactions on HAT from the C–H bonds of basic substrates such as tertiary alkylamines to the cumyloxy radical ( $PhC(CH_3)_2O^\bullet$ ,  $CumO^\bullet$ ).<sup>9,10</sup> Very large decreases in the rate constants for HAT from the  $\alpha$ -C–H bonds ( $k_H$ ) have been observed following nitrogen protonation or complexation by  $Mg^{2+}$ , conditions under which only an upper limit to  $k_H$  could be obtained. This behavior has been explained on the basis of the decrease in the degree of hyperconjugative overlap between the  $\alpha$ -C–H  $\sigma^*$  orbital and the nitrogen lone-pair determined by protonation or  $Mg^{2+}$ -complexation. This interaction increases the strength of the  $\alpha$ -C–H bonds leading to a destabilization of the HAT transition state and of the carbon centered radical formed after abstraction (Scheme 1, showing the effect of protonation on HAT from the  $\alpha$ -C–H of a generic tertiary alkylamine to  $CumO^\bullet$ ).

Support for this mechanistic picture has been recently provided by a computational study where it was shown that interaction between  $Mg^{2+}$  and the nitrogen lone pair of triethylamine leads to a 5.1 kcal mol<sup>–1</sup> increase in the  $\alpha$ -C–H bond dissociation energy (BDE) and to a greater than 4 order of magnitude decrease in  $k_H$ .<sup>11</sup>

## Scheme 1



Through the study of the effect of trifluoroacetic acid (TFA) on the reactions of  $CumO^\bullet$  with 1,4-dimethylpiperazine, an evaluation of the C–H deactivation determined by sequential protonation of one or both nitrogen centers has been also obtained,<sup>10</sup> showing that deactivation is not limited to the  $\alpha$ -C–H bonds but also extends to more remote positions. Taken together, the results of these studies have clearly shown that Brønsted and Lewis acid–base interactions can provide an extremely efficient method for the deactivation of otherwise strongly activated C–H bonds, allowing for control over the HAT selectivity.

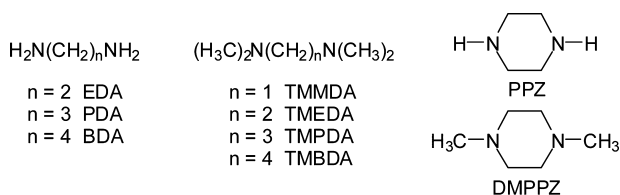
Along this line, in order to obtain additional information on these important aspects, we have carried out a detailed time-resolved kinetic study in MeCN and DMSO on the effect of

Received: April 15, 2014

Published: May 28, 2014

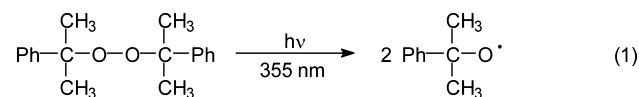
TFA on the reactions of CumO<sup>•</sup> with a series of substrates differing in both the number of activated  $\alpha$ -C–H bonds and the distance between the two basic centers, namely, primary and tertiary 1,*n*-alkanediamines (R<sub>2</sub>N(CH<sub>2</sub>)<sub>n</sub>NR<sub>2</sub>, R = H, CH<sub>3</sub>; *n* = 1–4), piperazine (PPZ), and 1,4-dimethylpiperazine (DMPPZ), whose structures are displayed in Chart 1. As a matter of comparison, the reactions of CumO<sup>•</sup> with *N,N*-dimethylbutanamine in MeCN and with triethylamine in DMSO have been also studied.

Chart 1



## RESULTS AND DISCUSSION

CumO<sup>•</sup> has been generated by 355 nm laser flash photolysis (LFP) of argon-saturated solutions (*T* = 25 °C) containing 1.0 M dicumyl peroxide (eq 1).



In MeCN and DMSO, CumO<sup>•</sup> is characterized by an absorption band in the visible region of the spectrum centered at 485 nm.<sup>12,13</sup> The C–H bonds of both solvents are strongly deactivated toward reaction with an electrophilic radical such as CumO<sup>•</sup> ( $k_{\text{H}}(\text{MeCN}) < 10^4 \text{ M}^{-1} \text{ s}^{-1}$ , and  $k_{\text{H}}(\text{DMSO}) = 1.8 \times 10^4 \text{ M}^{-1} \text{ s}^{-1}$ ),<sup>14–16</sup> and accordingly in these solvents the decay of CumO<sup>•</sup> reflects almost exclusively C–CH<sub>3</sub>  $\beta$ -scission.<sup>12,15</sup>

The reactions of CumO<sup>•</sup> with the substrates displayed in Chart 1 have been studied employing the LFP technique. It is well established that with tertiary alkylamines these reactions proceed by HAT from the  $\alpha$ -C–H bonds.<sup>17,18</sup> With primary and secondary alkylamines competition between  $\alpha$ -C–H and N–H abstraction is observed, with the former pathway being generally favored over the latter one.<sup>17</sup>

The time-resolved kinetic studies have been carried out following the decay of the CumO<sup>•</sup> visible absorption band at 490 nm as a function of substrate concentration. In the experiments carried out in the presence of TFA, fixed concentrations of acid have been employed: [TFA] = 80 mM in the reactions with EDA, PDA, and BDA, and [TFA] = 20–30 mM in the reactions with the other diamines. Under these conditions, the limited solubility displayed by EDA, BDA, and PPZ in MeCN limited the study of the effect of TFA on the reactions of CumO<sup>•</sup> with these substrates to DMSO.

With all substrates, excellent linear relationships have been obtained when the observed rate constants ( $k_{\text{obs}}$ ) have been plotted against substrate concentration and the second-order rate constants for HAT from the substrates to CumO<sup>•</sup> ( $k_{\text{H}}$ ) have been obtained from the slopes of these plots. The plots for HAT from 1,*n*-alkanediamines, PPZ, and DMPPZ to CumO<sup>•</sup> are displayed in the Supporting Information (SI, Figures S1–S6 and S8–S16). The  $k_{\text{H}}$  values thus obtained in MeCN and DMSO are collected in Tables 1 and 2, respectively. Also included in these tables are the kinetic data obtained for

reaction of CumO<sup>•</sup> with these substrates in the presence of TFA (see below).

**Table 1. Second-Order Rate Constants ( $k_{\text{H}}$ ) for Reaction of the Cumyloxyl Radical (CumO<sup>•</sup>) with 1,*n*-Alkanediamines, Measured in MeCN, in the Presence of TFA<sup>a</sup>**

substrate	[TFA]	$k_{\text{H}}/\text{M}^{-1} \text{ s}^{-1}$
EDA <sup>b</sup>	-	$(2.68 \pm 0.02) \times 10^7$
PDA	-	$(3.53 \pm 0.03) \times 10^7$
		no reaction for [PDA] $\leq$ 1/2 [TFA]
	80 mM	$k_{\text{H1}} = 1.30 \times 10^7$ for 1/2 [TFA] < [PDA] $\leq$ [TFA] $k_{\text{H2}} = 3.61 \times 10^7$ for [PDA] > [TFA]
BDA <sup>b</sup>	-	$(3.0 \pm 0.1) \times 10^7$
TMMDA	-	$(1.57 \pm 0.05) \times 10^8$
		no reaction for [TMMDA] $\leq$ 1/2 [TFA]
	30 mM	$k_{\text{H1}} = 3.37 \times 10^7$ for 1/2 [TFA] < [TMMDA] $\leq$ [TFA] $k_{\text{H2}} = 1.30 \times 10^8$ for [TMMDA] > [TFA]
TMEDA	-	$(2.44 \pm 0.09) \times 10^8$
		no reaction for [TMEDA] $\leq$ 1/2 [TFA]
	30 mM	$k_{\text{H1}} = 1.33 \times 10^8$ for 1/2 [TFA] < [TMEDA] $\leq$ [TFA] $k_{\text{H2}} = 2.46 \times 10^8$ for [TMEDA] > [TFA]
TMPDA	-	$(2.53 \pm 0.02) \times 10^8$
		no reaction for [TMPDA] $\leq$ 1/2 [TFA]
	30 mM	$k_{\text{H1}} = 1.32 \times 10^8$ for 1/2 [TFA] < [TMPDA] $\leq$ [TFA] $k_{\text{H2}} = 1.91 \times 10^8$ for [TMPDA] > [TFA]
TMBDA	-	$(2.64 \pm 0.04) \times 10^8$
		no reaction for [TMBDA] $\leq$ 1/2 [TFA]
	20 mM	$k_{\text{H1}} = 1.86 \times 10^8$ for 1/2 [TFA] < [TMBDA] $\leq$ [TFA] $k_{\text{H2}} = 2.46 \times 10^8$ for [TMBDA] > [TFA]
PPZ <sup>b</sup>	-	$(2.26 \pm 0.01) \times 10^{8c}$
DMPPZ	-	$(1.16 \pm 0.04) \times 10^{8d}$
		no reaction up to [DMPPZ] = 12 mM
	24 mM <sup>e</sup>	$k_{\text{H1}} = 1.34 \times 10^7$ for 1/2 [TFA] < [DMPPZ] $\leq$ [TFA] $k_{\text{H2}} = 1.11 \times 10^8$ for [DMPPZ] > [TFA]

<sup>a</sup>Measured in argon-saturated solution at *T* = 25 °C employing 355 nm LFP: [dicumyl peroxide] = 1.0 M.  $k_{\text{H}}$  values have been determined from the slope of the  $k_{\text{obs}}$  vs [substrate] plots, where in turn  $k_{\text{obs}}$  values have been measured following the decay of the CumO<sup>•</sup> visible absorption band at 490 nm. <sup>b</sup>Formation of a precipitate is observed after addition of TFA. <sup>c</sup>ref 19. <sup>d</sup>ref 20. <sup>e</sup>ref 10.

Starting from the experiments carried out in MeCN, the results displayed in Table 1 show that the  $k_{\text{H}}$  values measured for the primary (between 2.68 and  $3.53 \times 10^7 \text{ M}^{-1} \text{ s}^{-1}$ ) and tertiary 1,*n*-alkanediamines (between  $1.57$  and  $2.64 \times 10^8 \text{ M}^{-1} \text{ s}^{-1}$ ) are in line with the values measured previously under analogous experimental conditions for HAT from primary alkylamines to CumO<sup>•</sup> ( $k_{\text{H}} = 1.04 \times 10^7$  and  $1.8 \times 10^7 \text{ M}^{-1} \text{ s}^{-1}$ , for propylamine and butylamine, respectively),<sup>17</sup> and with the value measured in this study for HAT from *N,N*-dimethylbutanamine to CumO<sup>•</sup> in MeCN ( $k_{\text{H}} = (1.41 \pm 0.02) \times 10^8 \text{ M}^{-1} \text{ s}^{-1}$ , the plot for which is displayed in the SI as Figure S7). The up to 2-fold increase in  $k_{\text{H}}$  observed going from the amines to the diamines is in line with statistical factors as the latter substrates are characterized by a double number of  $\alpha$ -C–H bonds as compared to the former ones. Among the two series, the relatively lower  $k_{\text{H}}$  values measured with EDA and TMMDA can be explained on the basis of the electron withdrawing effect exerted by the remote nitrogen atom that, in

**Table 2. Second-Order Rate Constants ( $k_H$ ) for Reaction of the Cumyloxy Radical (CumO $\cdot$ ) with 1,*n*-Alkanediamines, Measured in DMSO, in the Presence of TFA**

substrate	[TFA]	$k_H/M^{-1} s^{-1}$
EDA	-	$(4.14 \pm 0.01) \times 10^7$ no reaction for [EDA] $\leq$ 1/2 [TFA]
	80 mM	$k_{H1} = 1.46 \times 10^7$ for $1/2 [TFA] \leq [EDA] \leq [TFA]$ $k_{H2} = 4.53 \times 10^7$ [EDA] > [TFA]
PDA	-	$(5.22 \pm 0.04) \times 10^7$ no reaction for [PDA] $\leq$ 1/2 [TFA]
	80 mM	$4.26 \times 10^7$ for [PDA] > 1/2 [TFA]
BDA	-	$(4.53 \pm 0.05) \times 10^7$ no reaction for [BDA] $\leq$ 1/2 [TFA]
	80 mM	$3.84 \times 10^7$ for [BDA] > 1/2 [TFA]
TMMDA	-	$(2.16 \pm 0.09) \times 10^8$ no reaction for [TMMDA] $\leq$ 1/2 [TFA]
	20 mM	$k_{H1} = 6.82 \times 10^7$ for $1/2 [TFA] < [TMMDA] \leq [TFA]$ $k_{H2} = 1.53 \times 10^8$ for [TMMDA] > [TFA]
TMEDA	-	$(3.44 \pm 0.02) \times 10^8$ no reaction for [TMEDA] $\leq$ 1/2 [TFA]
	20 mM	$k_{H1} = 1.11 \times 10^8$ for $1/2 [TFA] < [TMEDA] \leq [TFA]$ $k_{H2} = 3.00 \times 10^8$ for [TMEDA] > [TFA]
TMPDA	-	$(3.41 \pm 0.07) \times 10^8$ no reaction for [TMPDA] $\leq$ 1/2 [TFA]
	20 mM	$2.54 \times 10^8$ for [TMPDA] > [TFA]
TMBDA	-	$(3.40 \pm 0.01) \times 10^8$ no reaction for [TMBDA] $\leq$ 1/2 [TFA]
	20 mM	$2.76 \times 10^8$ for [TMBDA] > [TFA]
PPZ	-	$(3.0 \pm 0.1) \times 10^8$ no reaction for [PPZ] $\leq$ 1/2 [TFA]
	30 mM	$k_{H1} = 7.64 \times 10^7$ $1/2 [TFA] < [PPZ] \leq [TFA]$ $k_{H2} = 1.58 \times 10^8$ for [PPZ] > [TFA]
DMPPZ	-	$(1.89 \pm 0.04) \times 10^8$ no reaction for [DMPPZ] $\leq$ 1/2 [TFA]
	24 mM	$k_{H1} = 2.03 \times 10^7$ for [DMPPZ] $\leq$ [TFA] $k_{H2} = 2.30 \times 10^8$ for [DMPPZ] > [TFA]

<sup>a</sup>Measured in argon-saturated solution at  $T = 25$  °C employing 355 nm LFP; [dicumyl peroxide] = 1.0 M.  $k_H$  values have been determined from the slope of the  $k_{obs}$  vs [substrate] plots, where in turn  $k_{obs}$  values have been measured following the decay of the CumO $\cdot$  visible absorption band at 490 nm.

the reaction with an electrophilic radical such as CumO $\cdot$ , leads to a slight deactivation of the C–H bonds that are  $\alpha$  to the other nitrogen atom, deactivation that decreases with increasing the distance between the two nitrogen centers.

When HAT from PDA, TMMDA, TMEDA, TMPDA, and TMBDA to CumO $\cdot$  has been studied in MeCN solutions containing TFA (between 20 and 80 mM), a very similar behavior has been observed for all substrates (Figures S18–S21 in the SI). No significant increase in  $k_{obs}$  has been measured up to [substrate]  $\cong$  1/2[TFA]. A linear increase in  $k_{obs}$  has been then observed for  $1/2[TFA] < [substrate] \leq [TFA]$  and, with a different slope, for [substrate] > [TFA]. The  $k_{H1}$  and  $k_{H2}$  values obtained from the slopes of these plots in these concentration ranges are displayed in Table 1. As an example, the plots of  $k_{obs}$  vs [substrate] for the reactions of CumO $\cdot$  with PDA in MeCN containing 80 mM TFA are shown in Figure 1 (black circles). As a matter of comparison, the  $k_{obs}$  vs [PDA] plot obtained for reaction of CumO $\cdot$  with PDA in MeCN in the absence of TFA has also been included in Figure 1 (white circles).

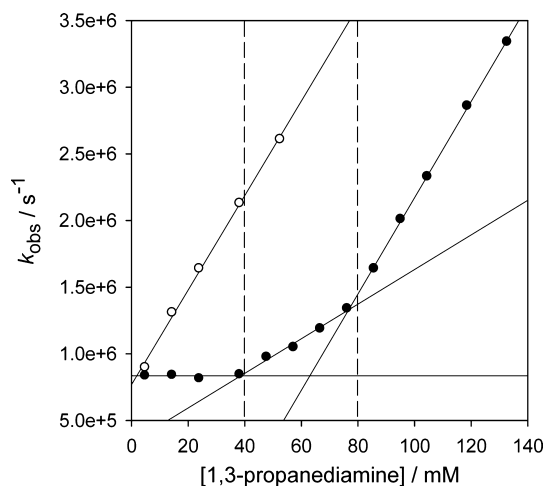
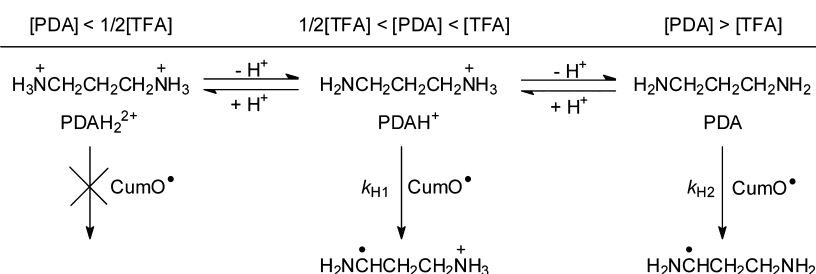


**Figure 1.** Plots of the observed rate constant ( $k_{obs}$ ) against [PDA] for reaction of the cumyloxy radical (CumO $\cdot$ ) measured at  $T = 25$  °C in an argon-saturated MeCN solution (white circles) and in an argon-saturated MeCN solution containing 80 mM trifluoroacetic acid (TFA) (black circles), by following the decay of CumO $\cdot$  at 490 nm. From the linear regression analysis: MeCN:  $k_H = 3.55 \times 10^7 M^{-1} s^{-1}$ ,  $r^2 = 0.9980$ . MeCN + 80 mM TFA: in the 40–80 mM [PDA] range:  $k_{H1} = 1.30 \times 10^7 M^{-1} s^{-1}$ ,  $r^2 = 0.9793$ ; in the 80–132 mM [PDA] range:  $k_{H2} = 3.61 \times 10^7 M^{-1} s^{-1}$ ,  $r^2 = 0.9995$ . The dashed lines highlight [PDA] of 40 and 80 mM.

An identical behavior has been observed previously when the reaction between CumO $\cdot$  and DMPPZ has been studied in MeCN containing 24 mM TFA,<sup>10</sup> and has been explained on the basis of the effect of sequential protonation of the DMPPZ nitrogen atoms by TFA on the HAT reactivity, showing that in MeCN TFA is sufficiently strong as an acid to protonate quantitatively both nitrogen centers of DMPPZ. Along these lines, the present results can be explained accordingly on the basis of the sequential protonation equilibria of the diamines  $R_2N(CH_2)_nNR_2$  ( $R = H, CH_3$ ), as shown in Scheme 2 taking PDA as a representative example, indicating that in MeCN TFA can also protonate both nitrogen centers of PDA, TMMDA, TMEDA, TMPDA, and TMBDA.<sup>21</sup>

At [substrate]  $\leq$  1/2[TFA], the diamine exists exclusively in its doubly protonated form  $HR_2N^+(CH_2)_nN^+R_2H$ , strong deactivation of the  $\alpha$ -C–H bonds occurs, and no reaction with CumO $\cdot$  is observed, in line with the greater than 4 orders of magnitude decrease in  $k_H$  that has been recently observed in the reactions between CumO $\cdot$  and tertiary alkylamines following protonation.<sup>10</sup> At [substrate] > 1/2[TFA],  $HR_2N^+(CH_2)_nN^+R_2H$  equilibrates with  $R_2N(CH_2)_nNR_2$  and both species are converted into the monoprotonated form  $R_2N(CH_2)_nN^+R_2H$  that reaches its maximum concentration at [substrate] = [TFA]. As nitrogen protonation strongly deactivates the adjacent C–H bonds, the increase in  $k_{obs}$  observed by increasing [substrate] in this concentration range ( $1/2[TFA] < [substrate] \leq [TFA]$ ), quantified by the  $k_{H1}$  value, reflects HAT from the C–H bonds that are  $\alpha$  to the nonprotonated nitrogen in  $R_2N(CH_2)_nN^+R_2H$ . At [substrate] > [TFA]  $k_{H2}$  values that are very close to those measured in the absence of added acid have been obtained, indicating that the linear increase in  $k_{obs}$  observed under these conditions reflects HAT from the  $\alpha$ -C–H bonds of the neutral substrate  $R_2N(CH_2)_nNR_2$ . Thus, comparison between the  $k_{H1}$  and  $k_{H2}$  values displayed in Table 1 provides a quantitative evaluation of the deactivation of the C–H bonds that are  $\alpha$  to a nitrogen

Scheme 2

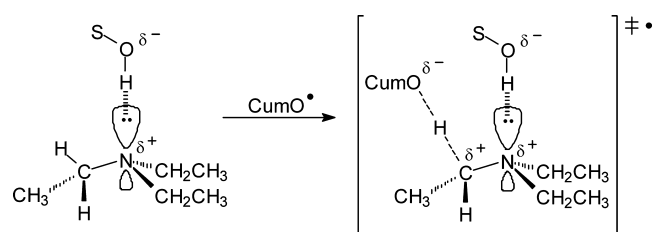


atom determined by protonation of the remote nitrogen atom. Along this line the  $\sim 3$ -fold decrease in the  $k_{\text{H2}}/k_{\text{H1}}$  ratio observed along the tertiary  $1,n$ -alkanediamine series on going from TMMDA (for which  $k_{\text{H2}}/k_{\text{H1}} = 3.86$ ) to TMBDA (for which  $k_{\text{H2}}/k_{\text{H1}} = 1.32$ ) reflects the increased distance between the positive charge and the activated  $\alpha$ -C–H bonds.

Moving then to the results of the experiments carried out in DMSO, comparison between the data displayed in Tables 1 and 2 clearly shows that for all the substrates investigated the  $k_{\text{H}}$  values increase on going from MeCN to DMSO, with  $k_{\text{H(DMSO)}}/k_{\text{H(MeCN)}}$  ratios that vary between 1.3 and 1.6. To the best of our knowledge these represent the first rate constant values measured in DMSO for HAT from the  $\alpha$ -C–H bonds of alkylamines to alkoxy radicals.

Solvent effects on HAT from triethylamine to  $\text{CumO}^\bullet$  have been studied in detail,<sup>23</sup> and a  $\sim 7$ -fold decrease in  $k_{\text{H}}$  has been measured on going from isooctane to MeOH (for which  $k_{\text{H}} = 2.9 \times 10^8$ ,<sup>20</sup> and  $3.8 \times 10^7 \text{ M}^{-1} \text{ s}^{-1}$ ,<sup>23</sup> respectively), i.e., on increasing the solvent hydrogen bond donor (HBD) ability. This behavior has been explained on the basis of polar contributions to the transition state and of overlap between the  $\alpha$ -C–H bond and the nitrogen lone pair. It has been suggested that the HAT transition state is characterized by a certain extent of charge separation with the development of a partial negative charge on the cumyloxy oxygen atom and a partial positive charge on the incipient carbon centered radical as described in Scheme 1.<sup>14</sup> Solvent hydrogen bonding to nitrogen determines a decrease in electron density at the incipient radical center leading to a destabilization of the transition state as compared to non-HBD solvents (Scheme 3, where SOH represents a generic HBD solvent).

Scheme 3



In keeping with the effect of protic acids shown in Scheme 1 and discussed above, this hydrogen bond interaction also decreases the degree of hyperconjugative overlap between the  $\alpha$ -C–H  $\sigma^*$  orbital and the lone-pair, leading to an increase in the strength of this bond and to a destabilization of the HAT transition state and of the carbon centered radical formed after abstraction. On the basis of this picture, the increase in  $k_{\text{H}}$  observed on going from MeCN to DMSO can be explained in terms of the greater HBD ability of MeCN as compared to

DMSO (as measured by Abraham's  $\alpha_2^{\text{H}}$  parameters:  $\alpha_2^{\text{H}} = 0.09$  and 0.00 for MeCN and DMSO,<sup>24</sup> respectively). As a matter of comparison, the reaction between  $\text{CumO}^\bullet$  and triethylamine has been also studied in DMSO (the plot for which is displayed in the SI as Figure S17) leading to a value  $k_{\text{H}} = (2.55 \pm 0.05) \times 10^8 \text{ M}^{-1} \text{ s}^{-1}$ , that is again higher than the value measured previously in MeCN ( $k_{\text{H}} = 2.19 \times 10^8 \text{ M}^{-1} \text{ s}^{-1}$ ).<sup>23</sup> Interestingly, despite of the very different solvent properties, the  $k_{\text{H}}$  value measured in DMSO is very close to the values measured previously in benzene and chlorobenzene ( $k_{\text{H}} = 2.8 \times 10^8$  and  $2.7 \times 10^8 \text{ M}^{-1} \text{ s}^{-1}$ ,<sup>23</sup> respectively), clearly indicating that the kinetic solvent effects observed in HAT reactions from alkylamines are mostly governed by the solvent HBD ability.

HAT from the substrates displayed in Chart 1 to  $\text{CumO}^\bullet$  has been then studied in DMSO solutions containing TFA (between 20 and 80 mM). With EDA, TMMDA, TMEDA, and PPZ a behavior that is very similar to the one described above for the reactions in MeCN has been observed (Figures S22, S25, and S28 in the SI, showing the  $k_{\text{obs}}$  vs [substrate] plots). No significant variation in  $k_{\text{obs}}$  has been measured up to [substrate]  $\cong 1/2[\text{TFA}]$ . A linear increase in  $k_{\text{obs}}$  has then been observed for  $1/2[\text{TFA}] < [\text{substrate}] \leq [\text{TFA}]$  and, with a different slope, for [substrate]  $> [\text{TFA}]$ . The  $k_{\text{H1}}$  and  $k_{\text{H2}}$  values thus obtained are displayed in Table 2. A different behavior has been instead observed in the reactions of PDA, BDA, TMPDA, and TMBDA (Figures S23, S24, S26, and S27 in the SI, showing the  $k_{\text{obs}}$  vs [substrate] plots) where no significant increase in  $k_{\text{obs}}$  has been measured up to [substrate]  $\cong 1/2[\text{TFA}]$ , while a linear increase in  $k_{\text{obs}}$  has been then observed for [substrate]  $> 1/2[\text{TFA}]$  with no change in slope being observed for [substrate]  $> [\text{TFA}]$ . The  $k_{\text{H}}$  values thus obtained are also displayed in Table 2. Two representative examples of these different behaviors are provided by Figure 2, where the  $k_{\text{obs}}$  vs [substrate] plots for the reactions of  $\text{CumO}^\bullet$  with TMEDA (black circles) and TMBDA (white circles) in DMSO containing 20 mM TFA are displayed.

The behavior observed in the reactions with EDA, TMMDA, TMEDA, and PPZ can be explained in terms of the sequential protonation equilibria described above (Scheme 2), clearly indicating that also in DMSO TFA is sufficiently strong as an acid ( $\text{p}K_{\text{a}}(\text{DMSO}) = 3.45$ )<sup>22</sup> to quantitatively protonate both nitrogen centers of these substrates.

Although limited information is presently available on the basicity of alkylamines in DMSO,<sup>22</sup> and no data are available for  $1,n$ -alkanediamines, useful information in this respect can be obtained from the comparison of the available data with the corresponding  $\text{p}K_{\text{a}}$  values measured in water. It is well established that in water and DMSO alkylamines are characterized by similar  $\text{p}K_{\text{a}}$  values.<sup>25,26</sup> DMSO is a significantly stronger hydrogen bond acceptor (HBA) than water (as measured by Abraham's  $\beta_2^{\text{H}}$  parameters:  $\beta_2^{\text{H}} = 0.78$  and 0.38

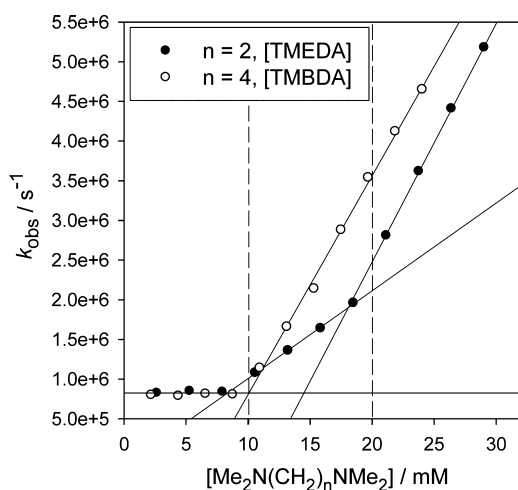


**Figure 2.** Plots of the observed rate constant ( $k_{\text{obs}}$ ) against  $[\text{Me}_2\text{N}(\text{CH}_2)_n\text{NMe}_2]$  for the reactions of the cumyloxyl radical ( $\text{CumO}^\bullet$ ) with TMEDA ( $n = 2$ , black circles) and TMBDA ( $n = 4$ , white circles) measured at  $T = 25^\circ\text{C}$  in an argon-saturated DMSO solution containing 20 mM trifluoroacetic acid (TFA), by following the decay of  $\text{CumO}^\bullet$  at 490 nm. From the linear regression analysis: TMEDA, in the 10–20 mM  $[\text{TMEDA}]$  range:  $k_{\text{H}} = 1.11 \times 10^8 \text{ M}^{-1} \text{ s}^{-1}$ ,  $r^2 = 0.9989$ ; in the 20–29 mM  $[\text{TMEDA}]$  range:  $k_{\text{H}} = 3.00 \times 10^8 \text{ M}^{-1} \text{ s}^{-1}$ ,  $r^2 = 0.9998$ . TMBDA, in the 10–24 mM  $[\text{TMBDA}]$  range:  $k_{\text{H}} = 2.76 \times 10^8 \text{ M}^{-1} \text{ s}^{-1}$ ,  $r^2 = 0.9970$ . The dashed lines highlight  $[\text{Me}_2\text{N}(\text{CH}_2)_n\text{NMe}_2]$  of 10 and 20 mM.

for DMSO and  $\text{H}_2\text{O}$ ,<sup>24</sup> respectively) and in this solvent the stabilization of an ammonium ion is expected to decrease by decreasing the number of hydrogens. Accordingly, in DMSO, within an alkylamine series, the  $\text{p}K_{\text{a}}$  values increase in the order tertiary < secondary < primary. Comparison between DMSO and water shows in particular that primary amines are stronger bases in DMSO than in water (for the corresponding ammonium ions  $\text{p}K_{\text{a}}(\text{DMSO}) - \text{p}K_{\text{a}}(\text{H}_2\text{O}) \sim 0.5$ ), whereas tertiary amines, that in the protonated form display a single N–H bond, are considerably weaker bases in DMSO than in water ( $\text{p}K_{\text{a}}(\text{H}_2\text{O}) - \text{p}K_{\text{a}}(\text{DMSO}) \sim 2$ ).<sup>25,26</sup> Along these lines, the availability of  $\text{p}K_{\text{a}}$  values for 1, $n$ -alkanediamines in water allows a reliable prediction of the corresponding  $\text{p}K_{\text{a}}$  values in DMSO.

As the  $\text{p}K_{\text{a}1}$  and  $\text{p}K_{\text{a}2}$  values of 1, $n$ -alkanediamines are known to increase with increasing  $n$ ,<sup>22,27,28</sup> the observation that TFA is able to protonate both nitrogen atoms of EDA, TMMDA, TMEDA, and PPZ (i.e., of the substrates characterized by the lowest numbers of  $\text{CH}_2$  units between the two nitrogens) clearly indicates that the same must also hold for PDA, BDA, TMPDA, and TMBDA, a hypothesis that is confirmed by the observation that in the reactions of these substrates with  $\text{CumO}^\bullet$  in DMSO containing TFA, no significant increase in  $k_{\text{obs}}$  has been measured up to  $[\text{substrate}] \cong 1/2[\text{TFA}]$ .

As mentioned previously, at  $[\text{substrate}] > 1/2[\text{TFA}]$ , the doubly protonated diamine  $\text{HR}_2\text{N}^+(\text{CH}_2)_n\text{N}^+\text{R}_2\text{H}$  ( $\text{R} = \text{H}, \text{CH}_3$ ) equilibrates with  $\text{R}_2\text{N}(\text{CH}_2)_n\text{NR}_2$  and both species are converted into the monoprotonated form  $\text{R}_2\text{N}(\text{CH}_2)_n\text{N}^+\text{R}_2\text{H}$ , with the result that in the  $1/2[\text{TFA}] < [\text{substrate}] \leq [\text{TFA}]$  range, for every added molecule of neutral diamine two molecules of the monoprotonated diamine are formed. Thus, for  $[\text{TFA}] = 20 \text{ mM}$ , the slope of the  $k_{\text{obs}}$  vs  $[\text{substrate}]$  plots in the 10–20 mM range should be divided by a factor of 2 to account for this equilibration. At  $[\text{substrate}] > [\text{TFA}]$ ,  $\text{R}_2\text{N}(\text{CH}_2)_n\text{N}^+\text{R}_2\text{H}$  is present at constant concentration that is equal to the concentration of TFA, and the slope of the  $k_{\text{obs}}$

vs  $[\text{substrate}]$  plot now reflects HAT from  $\text{R}_2\text{N}(\text{CH}_2)_n\text{NR}_2$ . Also in this case the slope should be divided by a factor 2 to account for the fact that as compared to  $\text{R}_2\text{N}(\text{CH}_2)_n\text{N}^+\text{R}_2\text{H}$ ,  $\text{R}_2\text{N}(\text{CH}_2)_n\text{NR}_2$  is characterized by a double number of activated  $\alpha\text{-C-H}$  bonds. On the basis of this picture, the linear increase in  $k_{\text{obs}}$  observed in the reactions of  $\text{CumO}^\bullet$  with PDA, BDA, TMPDA, and TMBDA in DMSO for  $[\text{substrate}] > 1/2[\text{TFA}]$  and extending to  $[\text{substrate}] > [\text{TFA}]$  clearly indicates that with these substrates the C–H bonds that are  $\alpha$  to the nonprotonated nitrogen in the monoprotonated diamine and the  $\alpha\text{-C-H}$  bonds of the neutral diamine display the same reactivity toward  $\text{CumO}^\bullet$ . In other words, it appears that in DMSO C–H deactivation is no longer observed when the protonated nitrogen center is separated from the neutral one by more than two  $\text{CH}_2$  units, in contrast with MeCN where a certain extent of remote C–H deactivation is still observed when the two centers are separated by four  $\text{CH}_2$  units. DMSO is characterized by a significantly higher HBA ability than MeCN ( $\beta_2^{\text{H}} = 0.78$  and  $0.44$ ,<sup>24</sup> respectively) and can stabilize more efficiently through hydrogen bonding the ammonium moiety thus reducing its electron withdrawing effect and explaining the different reactivity patterns observed in these two solvents.

The effect of TFA on the reaction of  $\text{CumO}^\bullet$  with DMPPZ, previously studied in MeCN,<sup>10</sup> has been also studied in DMSO, the plots for which are displayed in Figure 3.

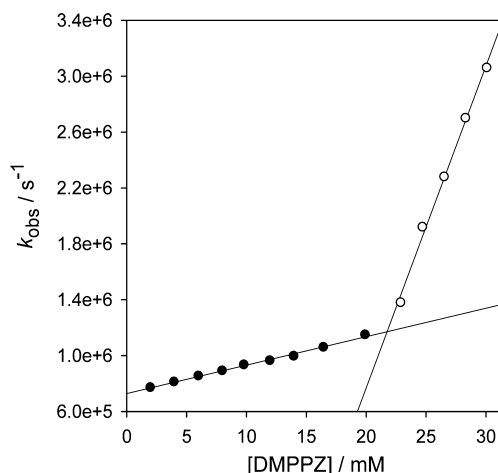


**Figure 3.** Plots of the observed rate constant ( $k_{\text{obs}}$ ) against the concentration of 1,4-dimethylpiperazine (DMPPZ) for reaction with the cumyloxyl radical ( $\text{CumO}^\bullet$ ) measured at  $T = 25^\circ\text{C}$  in an argon-saturated DMSO solution containing 24 mM trifluoroacetic acid (TFA), by following the decay of  $\text{CumO}^\bullet$  at 490 nm. From the linear regression analysis, in the 0–20 mM  $[\text{DMPPZ}]$  range (black circles):  $k_{\text{H}} = 2.03 \times 10^7 \text{ M}^{-1} \text{ s}^{-1}$ ,  $r^2 = 0.9942$ ; in the 23–30 mM  $[\text{DMPPZ}]$  range (white circles):  $k_{\text{H}} = 2.30 \times 10^8 \text{ M}^{-1} \text{ s}^{-1}$ ,  $r^2 = 0.9949$ .

In contrast with the results obtained with all the other substrates investigated, and with DMPPZ in MeCN,<sup>10</sup> where no significant variation in  $k_{\text{obs}}$  has been measured up to  $[\text{substrate}] \cong 1/2[\text{TFA}]$ ; under these conditions a linear increase in  $k_{\text{obs}}$  has been observed for  $[\text{DMPPZ}] \leq [\text{TFA}]$  (Figure 3, black circles) and, with a different slope, for  $[\text{DMPPZ}] > [\text{TFA}]$  (Figure 3, white circles). The  $k_{\text{H}1}$  and  $k_{\text{H}2}$  values obtained from the slopes of these plots are also displayed in Table 2. In aqueous solution, DMPPZ is characterized by the following  $\text{p}K_{\text{a}}$  values:  $\text{p}K_{\text{a}1} = 8.38$  and  $\text{p}K_{\text{a}2} = 3.81$ .<sup>29</sup> By taking into account that in DMSO tertiary amines are characterized by

$pK_a$  values that are lower by approximately 2 units than those measured in water,<sup>25,26</sup> it clearly appears that under these conditions double protonation of DMPPZ by TFA (for which  $(pK_a(\text{DMSO}) = 3.45)$  can occur to a limited extent, indicating that the  $k_{\text{H1}}$  value measured for  $[\text{DMPPZ}] \leq [\text{TFA}]$  ( $k_{\text{H1}} = 2.03 \times 10^7 \text{ M}^{-1} \text{ s}^{-1}$ ) reflects HAT from the monoprotonated form  $\text{DMPPZH}^+$ . At  $[\text{DMPPZ}] > [\text{TFA}]$  the slope of the  $k_{\text{obs}}$  vs  $[\text{DMPPZ}]$  plot now reflects HAT from the  $\alpha\text{-C-H}$  bonds of the neutral substrate DMPPZ, as confirmed by the observation that the  $k_{\text{H2}}$  value obtained in this concentration range ( $k_{\text{H2}} = 2.30 \times 10^8 \text{ M}^{-1} \text{ s}^{-1}$ ) is very similar to the value measured in DMSO in the absence of added acid ( $k_{\text{H}} = 1.89 \times 10^8 \text{ M}^{-1} \text{ s}^{-1}$ ). As compared to  $\text{DMPPZH}^+$ , DMPPZ is characterized by a double number of activated  $\alpha\text{-C-H}$  bonds, accordingly, after statistical correction, comparison between  $k_{\text{H1}}$  and  $k_{\text{H2}}$  shows that protonation of one basic site in DMPPZ leads to a 5-fold decrease in HAT reactivity. The different behavior observed in MeCN and DMSO can be instead explained on the basis of the inversion in the  $pK_a$  values for TFA and DMPPZ observed on going from the former solvent to the latter one.

In conclusion, the results obtained in this study clearly show that protonation of one or two nitrogen centers in diamines provides a very useful tool for selective C–H deactivation toward highly reactive oxygen centered radicals such as  $\text{CumO}^\bullet$ . Strong deactivation of the C–H bonds that are  $\alpha$  to a nitrogen center is obtained following protonation and under these conditions no reaction with  $\text{CumO}^\bullet$  is observed. Protonation of one basic center directs radical attack to the C–H bonds that are adjacent to the nonprotonated center that, however, as compared to the neutral substrate, are deactivated to a certain extent by the inductive effect of the remote positive charge. This remote C–H deactivation can be modulated by changing the number of methylene units between the two centers and by varying the solvent hydrogen bond acceptor ability. As C–H deactivation is the results of substrate protonation, similar effects should be also observed in HAT reactions from basic hydrogen atom donor substrates to other radicals and radical-like species. These aspects are currently under investigation in our laboratory.

## EXPERIMENTAL SECTION

**Materials.** Spectroscopic grade acetonitrile and DMSO were used in the kinetic experiments. 1,2-Ethanediamine (EDA), 1,3-propanediamine (PDA), 1,4-butanediamine (BDA),  $N,N,N',N'$ -tetramethylmethanediamine (TMMDA),  $N,N,N',N'$ -tetramethyl-1,2-ethanediamine (TMEDA),  $N,N,N',N'$ -tetramethyl-1,3-propanediamine (TMPDA),  $N,N,N',N'$ -tetramethyl-1,4-butanediamine (TMBDA), piperazine (PPZ), 1,4-dimethylpiperazine (DMPPZ), triethylamine, and  $N,N$ -dimethylbutanamine were of the highest commercial quality available and were used as received. The purity of the substrates was checked by GC prior to the kinetic experiments and was in all cases >99%. Trifluoroacetic acid (TFA) and dicumyl peroxide were of the highest commercial quality available ( $\geq 99\%$ ) and were used as received.

**Laser Flash Photolysis Studies.** LFP experiments were carried out with a laser kinetic spectrometer using the third harmonic (355 nm) of a Q-switched Nd:YAG laser, delivering 8 ns pulses. The laser energy was adjusted to  $\leq 10 \text{ mJ/pulse}$  by the use of the appropriate filter. A 3.5 mL Suprasil quartz cell (10 mm  $\times$  10 mm) was used in all experiments. Argon-saturated acetonitrile or DMSO solutions of dicumyl peroxide (1.0 M) were employed. In the experiments carried out in the presence of TFA fixed concentrations of acid were used ( $[\text{TFA}]$  between 20 and 80 mM). All the experiments were carried out at  $T = 25 \pm 0.5 \text{ }^\circ\text{C}$  under magnetic stirring. The observed rate constants ( $k_{\text{obs}}$ ) were obtained by averaging 2–5 individual values and were reproducible to within 5%. Second order rate constant for the

reactions of the cumyloxy radical with the different substrates in the absence or presence of TFA were obtained from the slopes of the  $k_{\text{obs}}$  (measured following the decay of the cumyloxy radical visible absorption band at 490 nm) vs  $[\text{substrate}]$  plots.

## ASSOCIATED CONTENT

### Supporting Information

Plots of  $k_{\text{obs}}$  vs  $[\text{substrate}]$  for the reactions of  $\text{CumO}^\bullet$ . This material is available free of charge via the Internet at <http://pubs.acs.org>.

## AUTHOR INFORMATION

### Corresponding Author

\*E-mail: [bietti@uniroma2.it](mailto:bietti@uniroma2.it)

### Notes

The authors declare no competing financial interest.

## ACKNOWLEDGMENTS

Financial support from the Ministero dell'Istruzione dell'Università e della Ricerca (MIUR) - PRIN 2010-2011 - project 2010PFLRJR (PROxi) is gratefully acknowledged. We thank Prof. Lorenzo Stella for the use of a LFP equipment and Prof. Miquel Costas for helpful discussions.

## REFERENCES

- (1) Iwasaki, K.; Wan, K. K.; Oppedisano, A.; Crossley, S. W. M.; Shenvi, R. A. *J. Am. Chem. Soc.* **2014**, *136*, 1300–1303.
- (2) (a) Gormisky, P. E.; White, M. C. *J. Am. Chem. Soc.* **2013**, *135*, 14052–14055. (b) Bigi, M. A.; Reed, S. A.; White, M. C. *J. Am. Chem. Soc.* **2012**, *134*, 9721–9726. (c) White, M. C. *Science* **2012**, *335*, 807–809. (d) Chen, M. S.; White, M. C. *Science* **2010**, *327*, 566–571. (e) Chen, M. S.; White, M. C. *Science* **2007**, *318*, 783–787.
- (3) (a) Prat, I.; Company, A.; Postils, V.; Ribas, X.; Que, L., Jr.; Luis, J. M.; Costas, M. *Chem.—Eur. J.* **2013**, *19*, 6724–6738. (b) Prat, I.; Gómez, L.; Canta, M.; Ribas, X.; Costas, M. *Chem.—Eur. J.* **2013**, *19*, 1908–1913. (c) Canta, M.; Font, D.; Prat, I.; Ribas, X.; Costas, M. *J. Org. Chem.* **2013**, *78*, 1421–1433. (d) Gómez, L.; Garcia-Bosch, I.; Company, A.; Benet-Buchholz, J.; Polo, A.; Sala, X.; Ribas, X.; Costas, M. *Angew. Chem., Int. Ed.* **2009**, *48*, 5720–5723.
- (4) Attouche, A.; Urban, D.; Beau, J.-M. *Angew. Chem., Int. Ed.* **2013**, *52*, 9572–9575.
- (5) Hitomi, Y.; Arakawa, K.; Kodera, M. *Chem.—Eur. J.* **2013**, *19*, 14697–14701.
- (6) Wei, W.-T.; Zhou, M.-B.; Fan, J.-H.; Liu, W.; Song, R.-J.; Liu, Y.; Hu, M.; Xie, P.; Li, J.-H. *Angew. Chem., Int. Ed.* **2013**, *52*, 3638–3641.
- (7) (a) Gephart, R. T., III; McMullin, C. L.; Sapiezynski, N. G.; Jang, E. S.; Aguila, M. J. B.; Cundari, T. R.; Warren, T. H. *J. Am. Chem. Soc.* **2012**, *134*, 17350–17353. (b) Wiese, S.; McAfee, J. L.; Pahls, D. R.; McMullin, C. L.; Cundari, T. R.; Warren, T. H. *J. Am. Chem. Soc.* **2012**, *134*, 10114–10121.
- (8) Michaudel, Q.; Thevenet, D.; Baran, P. S. *J. Am. Chem. Soc.* **2012**, *134*, 2547–2550.
- (9) Salamone, M.; Mangiacapra, L.; DiLabio, G. A.; Bietti, M. *J. Am. Chem. Soc.* **2013**, *135*, 415–423.
- (10) Salamone, M.; Giammarioli, I.; Bietti, M. *Chem. Sci.* **2013**, *4*, 3255–3262.
- (11) Nova, A.; Balcells, D. *Chem. Commun.* **2014**, *50*, 614–616.
- (12) Baciocchi, E.; Bietti, M.; Salamone, M.; Steenken, S. *J. Org. Chem.* **2002**, *67*, 2266–2270.
- (13) Avila, D. V.; Ingold, K. U.; Di Nardo, A. A.; Zerbetto, F.; Zgierski, M. Z.; Luszyk, J. *J. Am. Chem. Soc.* **1995**, *117*, 2711–2718.
- (14) Roberts, B. P. *Chem. Soc. Rev.* **1999**, *28*, 25–35.
- (15) Avila, D. V.; Brown, C. E.; Ingold, K. U.; Luszyk, J. *J. Am. Chem. Soc.* **1993**, *115*, 466–470.
- (16) Salamone, M.; DiLabio, G. A.; Bietti, M. *J. Org. Chem.* **2012**, *77*, 10479–10487.

- (17) Salamone, M.; DiLabio, G. A.; Bietti, M. *J. Am. Chem. Soc.* **2011**, *133*, 16625–16634.
- (18) Pischel, U.; Nau, W. M. *J. Am. Chem. Soc.* **2001**, *123*, 9727–9737.
- (19) Salamone, M.; Martella, R.; Bietti, M. *J. Org. Chem.* **2012**, *77*, 8556–8561.
- (20) Salamone, M.; DiLabio, G. A.; Bietti, M. *J. Org. Chem.* **2011**, *76*, 6264–6270.
- (21) In MeCN  $pK_{a1} = 19.7$ ,  $pK_{a2} = 14.9$  for PDA, and  $pK_a = 12.7$  for TFA.<sup>22</sup> To the best of our knowledge, no information is available on the basicity of tertiary 1,*n*-alkanediamines in this solvent.
- (22) Izutsu, K. *Acid-Base Dissociation Constants in Dipolar Aprotic Solvents*; Blackwell: Oxford, 1990.
- (23) Bietti, M.; Salamone, M. *Org. Lett.* **2010**, *12*, 3654–3657.
- (24) Abraham, M. H. *Chem. Soc. Rev.* **1993**, *22*, 73–83.
- (25) Crampton, M. R.; Robotham, I. A. *J. Chem. Res. (S)* **1997**, 22–23.
- (26) Kolthoff, I. M.; Chantooni, M. K., Jr.; Bhowmik, S. *J. Am. Chem. Soc.* **1968**, *90*, 23–28.
- (27) For example, in aqueous solution the following values are available for EDA, PDA, and BDA:  $pK_{a1} = 9.93$ , 10.30, and 10.50, and  $pK_{a2} = 6.85$ , 8.29, and 9.40, respectively.<sup>28</sup>
- (28) Perrin, D. D. *Dissociation Constants of Organic Bases in Aqueous Solution*; Butterworths: London, 1972.
- (29) Khalili, F.; Henni, A.; East, A. L. *J. Chem. Eng. Data* **2009**, *54*, 2914–2917.